UNIVERSITY OF PAVIA
FACULTY OF ENGINEERING

UNIVERSITY SCHOOL OF ADVANCED STUDIES - IUSS PAVIA

Evaluating the impact of climate change on the hydrology of the river Chiese

A Thesis Submitted in Partial Fulfilment of the Requirements

for the Degree of Master of Science (Laurea Magistrale) in

Civil Engineering for the Mitigation of Risk from Natural Hazards

by

Amin Minaei

Supervisor: Enrico Fortunato Creaco, Associate Professor, Civil Engineering and Architecture Department -Hydraulic and Environmental Engineering Section, University of Pavia

Co-supervisor: Sara Todeschini, Assistant Professor, Civil Engineering and Architecture Department -Hydraulic and Environmental Engineering Section, University of Pavia

September 2021

ABSTRACT

Climate change increasingly is affecting every aspect of human life on the earth. Many regional climate models (RCMs) have so far been developed to carefully assess this important phenomenon on specific regions. While many studies apply some post-processing actions to RCMs outputs such as interpolation (rescaling, remapping, and re-gridding) for matching the resolution of observations, this study proposes a novel approach that does not require any post-processing, resulting in the improvement of RCM evaluations. For this, 10 RCMs captured from the EURO CORDEX platform are evaluated on the river Chiese catchment located in the northeast of Italy, proving the Had-RCA4 RCM as the model with the overall best performance for precipitation and temperature simulation of the catchment. This model is then coupled with the hydrological model of Chiese catchment to assess the impacts of climate change. Three greenhouse gas emission scenarios, RCP (Representative Concentration Path for increase in the greenhouse gas emission) 2.6, 4.5, and 8.5, are considered in this context. The hydrological components of the catchment including discharge, percolation, and evapo-transpiration are calculated for and compared between historic (1991-2000) and future (2071-2080) decade simulations. The results show that catchment warming is obvious in all cases and therefore evapotranspiration will be intensified in the future. While rainfall events will feature higher intensity and shorter duration, there are slight increases in the yearly catchment precipitation depth. As the result of climate change, the catchment discharge and percolation components in 2071-2080 will be respectively higher and lower than those in 1991-2000.

Keywords: Climate change, regional climate model, specific region, evaluation, impact model, hydrological component

ACKNOWLEDGEMENTS

Throughout my life and the writing of this dissertation, I have received a great deal of support and assistance.

I would first like to thank my supervisor, Professor Enrico Creaco, whose expertise was invaluable in formulating the research questions and methodology. Your insightful feedback pushed me to sharpen my thinking and brought my work to a higher level. Moreover, I would like to thank the Co-supervisor of my thesis, Sara Todeschini, whose suggestions, and comments were always helpful for completing the thesis.

Secondly, I would love to thank my parents, Fariba and Mostafa, for their wise counsel and sympathetic ear. You are always there for me and the most valuable gift in my life. In addition, I would like to thank my lovely sisters, Elahe and Ailin, who are always a great source of inspiration and happiness to me. I am the luckiest to have you in my life.

My special thank is for my girlfriend, Maria, who proved me a genuine love. She was always beside me during my ups and downs when I was writing my thesis, something that I value forever. Additionally, I deeply send my appreciation to Maria's parents, Anna and Antonio for their unique hospitality and kindness to me, and her siblings, Giuseppe and his girlfriend Melissa, and Chiara who always intimately welcome me. I am so happy to have you in my life.

I would like to acknowledge my classmates, professors, colleagues, and directors from IUSS, UNIPV and my internship for the CE4WE project. Particularly, I would like to mention Prof. Sauro Manenti for his useful guidance, and Gianluca Colliva, Emily Alyssa Baker, Alessandro Cappato, and Wazita Scott for their wonderful collaboration throughout the project implementation.

I would also like to thank all my tutors over my whole academic life for their valuable guidance throughout my studies. I would particularly like to single out my previous supervisor, Prof. Ali Haghighi at Shahid Chamran University of Ahvaz for all his help and support. Finally, I would like to thank all my true friends particularly Dr. Adell Moradi Sabzkouhi who is always ready to provide stimulating discussions as well as happy distractions to rest my mind outside of my research.

TABLE OF CONTENTS

LIST OF FIGURES

LIST OF TABLES

LIST OF SYMBOLS

$x_{i,j}$ = Cumulative Monthly Precipitation of Month i and Year j

$y_{i,j}$ = Average Monthly temperature of Month i and Year j

$X_{i,j,catchment}$ = Weighted Average Catchment $x_{i,j}$

$Y_{i,j,catchment}$ = Weighted Average Catchment $y_{i,j}$

$RMSE^{P}_{i,catchment,z}$ = Root Mean Square Error of $X_{i,j,catchment}$ for Climate Model z

$RMSE^{T}_{i,catchment,z}$ = Root Mean Square Error of $Y_{i,j,catchment}$ for Climate Model z

$CM^{P}_{z,error}$ = Error of Climate Model z in Terms of Precipitation

$CM^{T}_{z,error}$ = Error of Climate Model z in Terms of Temperature

CM^{P}_{z,r_error} = Relative Error of Climate Model z in Terms of Precipitation

$\overline{(P^{y}_{E\text{-}OBS})_{i,catchment}}$ = Catchment Mean Precipitation of Month i over the Historic Period Captured from E-OBS (Daily Gridded Land Only Observational Dataset)

$\overline{(P^{y}_{CM})_{i,catchment}}$ = Catchment Mean Precipitation of Month i over the Historic Period Captured from a Climate Model

$\alpha_{P,i,catchment}$ = Bias Correction Factor for Catchment Month i Precipitation Data

$\overline{(T^{y}_{E\text{-}OBS})_{i,catchment}}$ = Catchment Mean Temperature of Month i over the Historic Period Captured from E-OBS (Daily Gridded Land Only Observational Dataset)

$\overline{(T^{y}_{CM})_{i,catchment}}$ = Catchment Mean Precipitation of Month i over the Historic Period Captured from a Climate Model

$\Delta T_{i,catchment}$ = Bias Correction Additive Term for Catchment Month i Temperature Data

$(P^{y}_{CM})'_{i,j,catchment}$ = Corrected Value Catchment Precipitation of Month i and Year j Related to Historic Period Captured from a Climate Model

$(T^{h}_{CM})'_{i,j,catchment}$ = Corrected Value Catchment Temperature of Month *i* and Year *j* Related to Historic Period Captured from a Climate Model

$(P^{f}_{CM})'_{i,j,catchment}$ = Corrected Value Catchment Precipitation of Month *i* and Year *j* Related to Future Period Captured from a Climate Model

$(T^{f}_{CM})'_{i,j,catchment}$ = Corrected Value Catchment Temperature of Month *i* and Year *j* Related to Future Period Captured from a Climate Model

$\Delta t_{\text{threshold}}$ = Inter Event Time Between Two Independent Rainfall Events

n = The Duration of a Rainfall Event (Hours)

t_0 = The Initial Time of a Rainfall Event

t_n = The End Time of a Rainfall Event

L_k = The Length of Rainfall Event *k* (hours)

D_k = The Depth of Rainfall Event *k* (mm)

I_k = The Intensity of Rainfall Event *k* (mm/hours)

1. INTRODUCTION

Climate change and its associated outcomes more than ever wreak havoc on the existence of life on Earth. This has drawn the attention of researchers in the field to accurately assess climate change and its impacts on every aspect of environment. The availability of water, one of the vital components of nature, is inextricably bound up with climate change. Therefore, this motivates the development of impact models concerning the hydrology of catchments. In this regard, many regional climate models (RCMs) have been developed, resulting from dynamical downscaling of global climate models (GCMs), to simulate future climate (precipitation, temperature, and other hydro-climatological variables) all over the world. The output of climate models is used as the input of the hydrological models to simulate the future hydrological behavior of the catchment in terms of evapotranspiration, percolation, runoff and so forth. While this is significant for decision makers in terms of launching adaptive plans against hydroclimatic hazards, there is always a debate about the functional accuracy of RCMs. In this regard, many experts in the area have introduced some methods for evaluating climate models' performance. To evaluate the performance of RCMs, the comparison of observations with RCM outputs is carried out. This represents a serious challenge as the resolution of numerical schemes of the models and observations are different. To overcome this, the dominant approach in many previous studies is to perform, the interpolation (re-gridding, and remapping) of the resolution of observations and model outputs to the same grid points.

While rescaling and remapping to fit the scheme of observations and models are well-established methods among the authors, this could alter the outputs due to the errors inherent in interpolation techniques. This should be carefully considered, as the RCMs are rescaled from GCMs, and the observations are the result of interpolated data from real gauges in many cases. Therefore, double interpolation could increase the systematic error in the evaluation of RCMs which could give a wrong view about the performance of an RCM for climate simulation of a specific case study. Similarly, the same error can be produced when interpolation is used to transfer data from an RCM grid points to the ones used for hydrological models. Furthermore, the comparison of models at fine spatial resolution could be affected by large errors as basically an output of a climate model (CM) represents the average value of an area, whereas an observation gives the value of one point related to a specific coordinate.

Another important issue in the process of RCMs evaluation and validation lies in the fact that grid points may have different levels of significance in the overall hydrological response of the catchment to climate change scenarios. In this regard, many studies compare the arithmetic mean values of model's outputs and observations over all respective grid points neglecting variations in the level of significance of grid points.

To overcome the two abovementioned limitations, this study aims to propose a novel method where the main strategy is to preserve climate model outputs when they are compared with observed data. This is done by carrying out this comparison at catchment level, resulting in a more realistic view of the performance of the various climate models and in the more accurate selection of the most suitable climate model for simulating the future hydrological behavior of a catchment. The method is applied to the Chiese catchment, located in the northeast of Italy, with an area of about $971 km^2$. To find the best climate model, an intercomparison is carried out between 10 RCMs captured from the Euro-CORDEX (European Coordinated Regional Climate Downscaling Experiment) framework and experimented in CMIP5 (Coupled Model Inter Comparison Project-Phase Five). Every native grid point of each RCM is considered as a fictitious meteorological station over the catchment and the weighted mean values of data on the RCMs grid points are compared with the weighted mean values of data on the observational grid points over the control period, 1971-2000 years. The method for calculating the weighted average of data is based on the Thiessen polygons technique. The meteorological variables are catchment cumulative monthly precipitation and average monthly two-meter land temperature values. Observations are daily gridded land-only datasets over Europe E-OBS transformed to monthly values for the purpose of comparison and evaluation. Root Mean Square Error (RMSE) index is used for ranking the models based on the error of estimated precipitation, and temperature. Finally, the best suited model to the case study, which is the one with the least total error rank (summation of monthly precipitation and temperature RMSE ranks) is chosen for coupling with the hydrological model, which is developed through the TOPographic Kinematic AProximation and Integration TOPKAPI (Liu and Todini 2002) software, which is a physically based distributed model. In the case study of the present work, TOPKAPI is applied with fine spatial and temporal resolutions. The hydrological model is calibrated for the period from 2010 to 2020 with the observed data including hourly precipitation and temperature, land use units, soil information, digital elevation model and discharge data at the outlet of the catchment. The output of the best rank RCM is used as input to the calibrated hydrological model with the final aim to assess the impacts of climate change on the future of hydrological variables including discharge, evapotranspiration, and percolation. Before applying the hydrological model, the outputs of the RCM are modified by a bias correction method. Then, four catchment hydrological simulations are carried out. The first is dedicated to simulating the decade 1991-2000 in the past while the three other simulations are addressed to simulating the future decade

2071-2080 with three RCP (Representative Concentration Path for Increase in the Greenhous Gas Emission) scenarios 2.6, 4.5 and 8.5, respectively. Finally, changes in the meteorological and hydrological variables for the future mentioned decade are assessed and compared with the results from the historic decade, 1991-2000.

2. LITRATURE REVIEW

Over the two last decades, many studies have been carried out concerning the performance assessment of downscaled RCMs together with the evaluation of impact models under climate change scenarios. While some of these studies assessed climate impact models through developing hydrological models, others only examined the impact of climate change scenarios on the meteorological-based data such as precipitation, temperature, and drought.

2.1 RCMS EVALUATION WITH DEVELOPING HYDROLOGICAL MODELS

As regards the coupling of RCMs with hydrological models, there are many studies in the scientific literature of the two most recent decades, including the following relevant studies.

Stone et al. (2001) assessed the changes in average daily cumulative reservoir storage, average annual flow of tributaries, seasonal water yield, monthly precipitation values, and monthly maximum temperature changes under conditions of doubled atmospheric carbon dioxide across the MISSOURI River catchment. The Soil and Water Assessment Tool (SWAT) rainfall-runoff model was used for simulating a physically based hydrological model consisting of 3949 sub catchments. They used one regional climate model with 50-km spatial grid resolution obtained from rescaling a GCM with $400km \times 500km$ spatial grid resolution. The RCM scheme was matched to the resolution of the hydrological model and the daily outputs of the RCM were transformed to monthly average values in order to be used by SWAT where representative precipitation was calculated for each catchment using the Thiessen polygons method (Wanielista 1990). They did not evaluate the performance of the RCM; however, they chose the well-established GCM, CISRO (Watterson et al. 1995) which had been developed at the time and obtained the RegCM (Regional climate model) through a downscaling method called nesting (Giorgi et al. 1998). They showed the impact of climate change through depicting the different hydrological responses from different locations in the catchment.

Kunstmann et al. (2004) showed the variation in the annual and seasonal precipitation, mean annual temperature, latent heat, and seasonal discharge values under one climate change scenario for an Alpine catchment. They employed a physically based distributed hydrological model (WaSiM) with the temporal and spatial resolutions of eight hours and

$100m \times 100m$, respectively. They evaluated the performance of a regional climate model downscaled from $2.8^{\circ} \times 2.8^{\circ}$ to $4 \times 4 km^2$ through comparing the results with outputs from another reanalyzed downscaled RCM which had coarser spatial resolution, $20 \times 20 km^2$. They compared the monthly aggregation of precipitation over all the grid points of the catchment where the grid points from two different resolutions were matched together using the attribution method based on the closest distance. To match the spatial resolution of RCM outputs with the hydrological model resolution, every grid point of the RCM was considered a fictitious station and they were interpolated to the WaSiM spatial resolution. The study focused on the significance of differences in the regional responses to climate change scenarios when a CM resolution gets finer.

Senatore et al. (2011) developed a physically based and fully distributed hydrological model (In-STRHyM) with temporal and spatial resolutions of one day and one kilometer, respectively. They assessed the changes in the average annual temperature, cumulative annual precipitation, snow accumulation, evapotranspiration, water stress, summer root zone soil moisture, groundwater storage, surface runoff under two scenarios for the Crati River catchment. Three RCMs with different spatial resolutions of 20-km, 0.11° and 0.165° were coupled with the hydrological model. For this, grid point (fictitious station) values of RCMs were interpolated to the resolution of In-STRHyM. The study emphasized that the output values of RCMs could have 50-100% error and therefore they should be modified before being used in the hydrological model. Hence, a bias correction method, captured from (Kunstmann et al. 2004), was used for modification and evaluation of RCMs outputs, where the aggregation of monthly precipitation values of all grid points from the model was divided into the grid points from the observational values within the control period. The temperature values were also modified through the subtraction of the model's total monthly temperatures from the corresponding observational temperatures over the control period. The interpolation error was mentioned as one of the inherent sources of error in the hydrological model calibration process.

Vezzoli et al. (2015) projected daily temperature and precipitation for the periods of 2041-2070 and 2071-2100 over the Po-river catchment to assess the impacts of climate change of two scenarios, RCP 4.5 and 8.5, on the climate and hydrology of the catchment. They used TOPKAPI software which simulated the hydrological process at a daily temporal resolution and a spatial resolution based on the resolution of the digital elevation model. They then coupled the climate model with the hydrological model and applied a uniform precipitation rate over the cells by means of the averaging method of Thiessen polygons. The target impact variables were the anomalies of seasonal and annual precipitation distributed (cell by cell) and averaged over the catchment respectively, whereas this was monthly-based scale for the discharge values at the outlet of the catchment. One RCM was considered in the study (about 8km horizontal resolution) and

its climatic outputs were modified before applying them to TOPKAPI. For this modification, distribution derived quantile mapping was employed as a bias correction method where daily precipitation values were considered for shaping the cumulative distribution functions (CDFs). The model outputs and observed data CDFs were compared, leading to the calculation of the bias correction factor through the transfer function (TF) matching of the mentioned CDFs at a monthly time scale. The TF parameters were estimated grid by grid where the interpolation of the model's grid points to observations' grid points was used for matching both resolution schemes.

Smiatek and Kunstmann (2019) used seven RCMs from EURO CORDEX to simulate future runoff in an alpine catchment and to assess the change in the future anomaly discharge under the climate change scenario RCP 4.5. For the coupling of RCMs with the hydrological model (WaSiM), the RCM numerical resolution was interpolated to WaSiM resolution where the RCM cell center points were considered as artificial monitoring stations. For the sake of RCMs evaluation, the observed reference (E-OBS) grids' resolution was remapped to the 0.25° resolution of the E-OBS dataset. The study highlighted errors in the CORDEX RCMs outputs even with a spatial resolution of about 12-km and further effort is needed for improving this deficiency particularly for the complex terrains found in such alpine catchments.

Peres et al. (2019) assessed the impacts of climate change scenarios on the precipitation, temperature, and runoff to simulate the effects on reservoir demand-performance curves of Pozzillo Reservoir in Sicily, Italy. They considered two scenarios, RCP 4.5 and 8.5, simulated by the best performing RCM model in the area. This was achieved using a ranking method where the high number of different RCM simulations were evaluated by measures of agreement with observed data, and then performing climate change impact assessment with those RCM data complying with certain accuracy requirements. In this approach, the performance of an RCM was evaluated through grid cell error evaluation estimated by comparison between annual average precipitation of the model and observations over the control period. Finally, the spatial average of errors over the all-grid cells was calculated as the index of model error. Peres et al. (2019) modified the monthly precipitation and temperature through the bias correction method proposed by Lenderink et al. (2007). According to this method, the RCM monthly precipitation data were corrected by multiplicative factors to bring the monthly means of corrected precipitation to their observed values. On the other hand, the temperature data were adjusted through an additive term to shift the corrected average monthly mean temperature towards the observed temperatures.

Tariku et al. (2021) used four GCMs dynamically downscaled by a regional climate model, Weather Research and Forecasting (WRF), for assessing the impacts of climate change on the extreme and mean streamflow of the Upper Blue Nile (UBN) simulated by three

hydrological models with different features. They considered two greenhouse gas emission scenarios, RCP 4.5 and 8.5 where the WRF was evaluated through the simulation accuracy of temperature, precipitation, shortwave, radiation against the similar ones obtained by gridded data of Global Precipitation Climatology Centre (GPCC), Climate Research Unit (CRU) and NCEP reanalysis data. The parameters of downscaling were adjusted to cover the target area with the spatial resolution of 36-km.

2.2 RCMS EVALUATION WITHOUT DEVELOPING HYDROLOGICAL MODELS

Besides the previously described state of the art, there are other studies focusing on the evaluation of climate and/or impact models without developing a hydrological model. Some of these studies are explained in the following paragraphs.

Frei et al. (2003) evaluated four RCMs and one GCM with a grid spacing of 50-km for the European Alps. Daily precipitation values were used to generate precipitation-based statistics including mean precipitation, wet-dry frequency, precipitation intensity and quantiles of the frequency distribution calculated at monthly, seasonal, and annual scales. They also introduced the approach of arithmetic mean statistics values over the domain for both the outputs of climate models and observations. These statistics were the base of the comparison between the results from the observational network and models. Observations were from high density rain gauges over the domain which were interpolated to the regular latitude and longitude grid points of climate models with the resolution of about $50km \times 50km$. The interpolation was carried out by weighting schemes which were based on distance from stations and directional clustering of stations around the analysis grid points of climate model. This was done to make the resolution of the models and observations compatible. There was the highlight that precipitation values from the climate model grid points represent the average of the computation grid boxes, while the station-based observed values underlying the point values influenced by site-specific conditions and therefore there is complication for the comparison and evaluation between CMs and observed data.

Schmidli et al. (2007) assessed six statistical downscaling models (SDMs) and three RCMs for the daily precipitation variable on the European Alps. They calculated seasonal index (SI) of some precipitation-based diagnostics such as climatological mean precipitation and wet dry frequency on the respective native grids of RCMs and then interpolated data to the common latitude-longitude grid with the rough resolution of $50km \times 50km$. The observations on the grid points were calculated using a similar method to that in (Frei et al. 2003). The mean values of the interannual average of the SI over all grid points of a subdomain together with the spatial correlation were the measures for the validation of climate models for different regions of the European Alps. They showed that analyses based on single grid points or even single stations are of very limited use in a highly

complex region since they create high uncertainties in the evaluation of the model's performance. Impact models included the change in the ratio of mean precipitation values between the future simulation and present measured values under only one emission scenario.

The desperate need for decision making on societal issues such as vulnerability and adaptation to a changing climate with weather/water extremes led to the numerous coordinated regional downscaling experiments (CORDEX) initiated by the World Climate Research Program (WCRP) in 2009. Together with advancements in scientific assessments on climate change made by the Intergovernmental Panel on Climate Change (IPCC), this has motivated many authors to evaluate the performance of CORDEX RCMs and the Impact Models (the impacts of climate models on the meteorological-based variables such as precipitation, temperature, and drought), used for climate modelling and research for the IPCC fifth assessment report (AR5) in 2014. In this regard, many contributions have been made where different climatic data and indexes as well as approaches were introduced for CORDEX RCMs, and Impact Models evaluation applied to different regions over the world (Table 2.1).

Table 2.1. Studies on Evaluation of RCMs and Impact Models within The CORDEX framework (without developing hydrological models)

References	Models	Comparison Variables	Impact Variables	Spatial Resolutions	Comparison Method
Endris et al. (2013)	10 RCMs from COREX Africa domain	Mean seasonal and annual precipitation together with the seasonal anomaly rainfall	-	~50-km (0.44°)	Observation and RCMs post processed to common grids had same spatial resolution. The variables were spatially averaged over every subregion and compared with the observed ones for the purpose of RCMs evaluation.
Kotlarski et al. (2014)	Nine Euro CORDEX RCMs	Mean seasonal temperature, precipitation, sea level pressure. Mean annual temperature, precipitation. Anomaly of mean seasonal and annual precipitation and temperature.	-	~12-km (0.11°), 50-km (0.44°)	Several grid-cell-by grid cell metrics were developed for model's evaluation. Hence, remapping of either the model's outputs or of E-OBS whose spatial resolution was 0.22° was done to the coarser

					spatial resolutions. The variables were arithmetically averaged over every subregion for the purpose of comparison.
Mascaro et al. (2015)	Six RCMs driven by 10 GCMs from CORDEX Africa domain	Accumulated mean annual precipitation. Accumulated mean annual evaporation. Accumulated mean annual water balance. Average monthly minimum temperature.	-	~50-km (0.44°)	All model and observation resolutions were regirded to match the codex domain. Arithmetically the temporal and spatial average of variables were calculated over the sub catchments for the purpose of comparison and evaluation of RCMs.
Park et al. (2016)	Five RCMs from the CORDEX East Asia Domain	Seasonal average daily mean temperature and precipitation. Seasonal maxima of daily mean temperature and precipitation.	-	~50-km (0.44°)	The dataset of RCMs was interpolated on to the same 0.5° × 0.5° grid resolution related to the observational dataset resolution and averaged arithmetically over the domain for the RCMs validation process.
Wu et al. (2016)	Four RCMs from RMIP project and their regional multi-model ensemble and their driving GCM ECHAM5 (Monsson Asia)	Average seasonal precipitation intensity. Percentage contribution of anomaly precipitation to total values. Maximum consecutive dry days.	Summer anomaly precipitation, Seasonal Consecutive dry days.	GCM with 1.875° × 1.875° , RCM with 0.5°×0.5°	All simulation results were interpolated to 0.5° × 0.5° for comparison purpose. The spatial distribution of variables was assessed and therefore there was not any domain spatial average.
Smiatek et al. (2016)	13 Euro CORDEX RCMs	Mean seasonal temperature and precipitation. Frequency distribution of precipitation intensity. Seasonal anomaly wet days.	Seasonal consecutive dry days. Mean seasonal precipitation and temperature.	~12-km (0.11°),	Evaluations of RCMs performances were carried out through remapping the RCMs resolutions to 0.25° which was the resolution of reference

					dataset, E-OBS. Area mean of variables was estimated arithmetically for understanding the spatial bias of models.
Um et al. (2017)	Four RCMs from CORDEX East Asia domain, their ensemble means, and a driving GCM	Drought characteristics based on the SPEI (Standard Precipitation Evapotranspiration Index) at seasonal and annual scale	-	RCMs with ~50-km (0.44°)	The spatial distribution of drought characteristics was calculated for both RCMs and observed data, where there were two different spatial resolutions. The resolutions were remapped to the common latitude and longitude grid points for the sake of comparison.
Diasso and Abiodun (2017)	10 RCMs from CORDEX Africa Domain	Seasonal drought characteristics evaluated through for principal components of SPEI	-	RCMs with ~50-km (0.44°)	All datasets were re-gridded into the CORDEX grid. To understand the spatial bias of models, the SPEI arithmetically was averaged over the domain.
Adeniyi and Dilau (2018)	10 RCMs from CORDEX Africa Domain	Precipitation, temperature, and drought (SPEI) anomaly with the temporal scales of three and six months	-	RCMs with ~50-km (0.44°)	They assessed the performance of RCMs through the correlation of models output with the observations (with resolution of $0.5^{\circ} \times 0.5^{\circ}$) remapped into the common grid points. Moreover, the arithmetic average of correlation coefficient of climatic data was calculated to evaluate spatial bias of models.
Foley and Kelman (2018)	Seven EURO-CORDEX RCMs and five driving GCMs	Several precipitation indices (accumulated precipitation amount, mean daily precipitation amount,	-	RCMs with ~12.5-km (0.11°)	Comparison was done in two phases: first, between modelled data and observations which had 5-km gridded

		maximum one- and five days precipitation amounts, simple daily intensity, number of heavy and very heavy precipitation days)			resolution. For this, the finer resolution observed data was interpolated to coarser grid of the models. In the second phase, station by station comparison was done where the modeled data were interpolated to the coordinates of stations.
Senatore et al. (2019)	Eight RCMs from CORDEX south Asian Domain	Annual and seasonal precipitation and temperature	Average seasonal temperature and precipitation	RCMs with ~50-km (0.44°)	After regarding the model datasets to the same domain and resolution ($0.5^{\circ} \times 0.5^{\circ}$) related to observations, the reliability of CORDEX models was evaluated by means of scatter plots. The root mean square errors (RMSE) were calculated for assessing models' performances. For this, the model's grid points values were compared by the closest corresponding ones from the observations.
Di Virgilio et al. (2019)	Six RCMs from CORDEX Australian domain	Near-surface max and min temperature and precipitation at annual, seasonal, and daily timescales	-	RCMs with ~50-km (0.44°)	All RCM data were interpolated from the models' native grid to a common regular 0.5° grid for comparison and analysis using a nearest neighbor algorithm. The observational dataset had much higher resolution than models (0.05°) and they were therefore re-gridded to correspond with the RCM data on a common 0.5° regular grid using the

					conservative area weighted re-gridding scheme. RMSE, average correlation and station by station probability distribution of data were the method of comparison.

Following the studies mentioned in the Table 2.1, Peres et al. (2020) carried out a comprehensive assessment on the performance of 19 EURO CORDEX RCMs (with the spatial resolution of 0.11°) in reproducing precipitation and temperature statistics along with drought characteristics. The study introduced a formula where models could be evaluated using a ranking method and eventually the performance of models for every property were compared. For the sake of comparison, the observational grid points were interpolated to the corresponding modelled grid points where the integration of variables over a domain was carried out arithmetically. In the study, average monthly Box plot and Taylor diagram tools were used to assess the performance of RCMs in terms of variables frequency occurrence and correlation over a domain. They showed that the robustness of a model in reproducing one climatic data (for example precipitation) does not guarantee the same performance for simulating other variables (temperature).

2.3 NOVELTY OF CURRENT STUDY

As explained, in all the contributions reported above there has been manipulation of the native numerical scheme of the climate models and/or of observations through interpolation (re-gridding, rescaling and remapping) techniques to match the resolutions of models and observational datasets for the purpose of comparison and evaluation. However, RCM outputs are affected by a systematic bias caused by, e.g., uncertainty in GCM/RCM parametrizations or assumptions, which has to be removed before performing quantitative evaluations on hydrological or other impacts (Teutschbein and Seibert 2010). Each of the components of the modelling process is a potential source of uncertainty that propagates through the process (Bosshard et al. 2013). Over the last decade, there has been an emphasis on the reduction of errors in the climate and hydrological fields (Chen et al. 2011, Ehret et al. 2012, Teutschbein and Seibert 2012, Brigode et al. 2013, Chen et al. 2015, Seaby et al. 2015, Van Uytven and Willems 2018, Mengistu et al. 2021). This has a great significance to policy makers for launching cost saving and accurate adaptive plans against high-impact water and climate disasters (Doss-Gollin et al. 2020). The present work takes inspiration from this research trend, proposing the comparison of RCM outputs and observations in the absence of interpolation on either source of data. Furthermore, the current study uses a hydrological impact assessment at a very fine temporal resolution (one hour), seldom explored in the

scientific literature, where the hydrological model and the RCM resolutions do not need to match each other for the coupling purpose.

3. DATA AND METHODS

3.1 STUDY AREA

The study area refers to the river Chiese Catchment where the Chiese mainstream has the length of about 121-km originating from Mount Adamello in Trentino region (Figure 4.3). The river Chiese is a large sub-tributary of the river Po, which is the longest river in Italy playing a major role in the economic development of the country in terms of various economic activities. The area and perimeter of catchment are roughly 971km^2 and 218-km respectively, and the catchment includes 18 and 15 real rain gauge and thermometer stations. These stations along with Gavardo hydrometer further contribute to hydrological analysis and calibration of river Chiese catchment for the estimation of hydrological variables of the catchment.

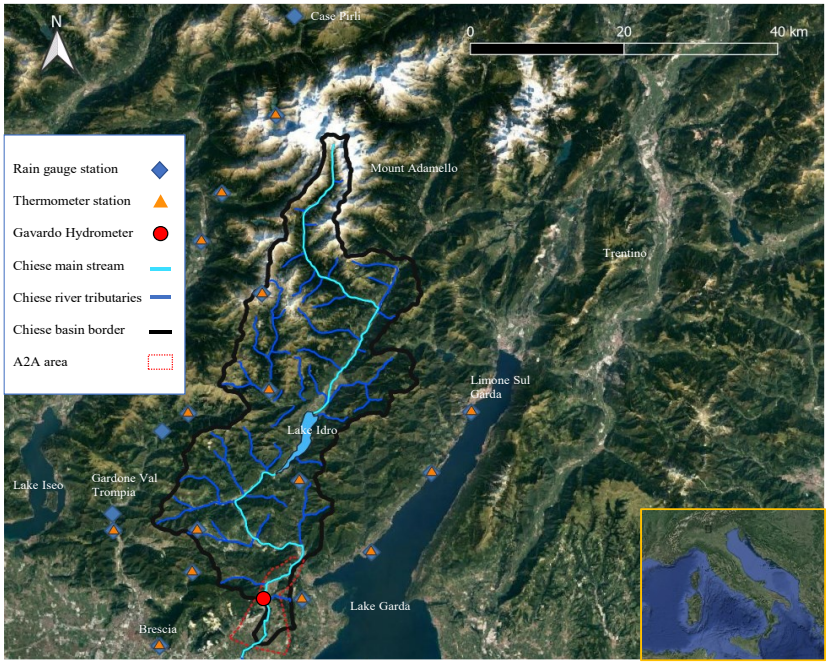

Figure 3.1. The river Chiese Catchment located in the northeast of Italy

3.2 DEVELOPING HYDROLOGICAL MODEL AND CALIBRATION

The river Chiese catchment is modeled through the software TOPKAPI enabling the user to set up a physically based and fully distributed hydrological model with the fine space-time resolution ((250m×250m) cell sizes and one hour time steps). To achieve this, various GIS-based information including shapefiles of the catchment area, the lakes, the river network, and the gauged stations (thermometers, rain gauges and hydrometers) together with Digital Elevation Models, map of soil and land use units are collected from different sources such as the environmental protection agency ARPA (https://www.arpalombardia.it/Pages/Ricerca-Dati-ed-Indicatori.aspx) and A2A water utility. The model is constructed in the GIS interface of TOPKAPI, MapWindow GIS where Preprocessor is used for inserting input data such as land use, soil parameters and monthly temperature values.

The model is divided into 15554 cells and TOPKAPI solves hydrologic cycle equations in every cell for every time step. A long-term hydrologic simulation, from 2010 to 2020, is carried out considering the real weather stations data are available at hourly resolution. TOPKAPI is able to represent all the components of the hydrological cycle: precipitation, discharge, percolation, evapotranspiration, channel, surface, soil, and snow water. Among them, the discharge at Gavardo hydrometer station is considered for the calibration of the model. The main adjustable parameters for calibrating the model are horizontal permeability, saturation and residual water content, and soil depth for each kind of soil. More information on TOPKAPI software, data, calibration process and results are provided in the Appendix.

3.3 CLIMATE MODELS

10 coupled climate models are investigated in the current study. The models are retrieved from the EURO-CORDEX CMIP5 (Coupled Model Intercomparison Project Phase Five) experiment (Jacob et al. 2014); https://www.euro-cordex.net/, stored on the nodes of Earth System Grid Federation (ESGF; https://esg-dn1.nsc.liu.se/login/).

The data are analyzed at the finest resolution, 0.11° (~12.5-km; EUR-11 referring to the models related to the European areas with the finest resolution) and considered for the historic period of 1971-2000 as a baseline. The used coupled Climate models are: CM5-RCA4, ECE-HIRH, ECE-RACM, ECE-RACMr12, ECE-RCA4, IPS-RCA4, Had-RACM, Had-RCA4, MPI-RCA4 and Nor-HIRH, which include three RCMs and six GCMs whose information is shown in Table 3.1 and Table 3.2 The ECE-RACMr12 refers to the same model of ECE-RACM with different realization (an ensemble experiment with different initial states from ECE-RACM).

Table 3.1. GCMs used in the current study and in EURO-CORDEX ensemble experiment

Model name	Abbreviation	Reference	Institution
CNRM-CERFACS-CNRM-CM5	CM5	Voldoire et al. (2013)	National Centre for Meteorological Research
ICHEC-EC-EARTH	ECE	Hazeleger et al. (2010)	Irish Centre for High-End Computing EC-Earth Consortium, Europe
IPSL-IPSL-CM5A-MR	IPS	Dufresne et al. (2013)	Institute Pierre Simon Laplace
MOHC-HadGEM2-ES	Had	Collins et al. (2011)	Met Office Hadley Centre
MPI-M-MPI-ESM-LR	MPI	Giorgetta et al. (2013)	Max Planck Institute for Meteorology
NCC-NorESM1-M	Nor	(Bentsen et al. 2013, Iversen et al. 2013)	Norwegian Earth System Model

Table 3.2. RCMs used in the current study and in EURO-CORDEX ensemble experiment

Model name	Abbreviation	Reference	Institution
SMHI-RCA4	RCA4	Strandberg et al. (2015)	Swedish Meteorological and Hydrological Institute, Rossby Centre
KNMI-RACM022E	RACM	van Meijgaard et al. (2008)	Royal Netherlands Meteorological Institute, De Bilt, the Netherlands
DMI-HRIHHAM5	HRIH	Christensen et al. (2007)	Danish Meteorological Institute

3.3.1 CMs Data Obtaining and Processing

A CM has a numerical scheme with horizontal grids where the physical quantities (e.g., temperature and precipitation) are stored on the grid points. The horizontal grid in the EURO CORDEX CMs has 106 and 103 grid points on the X and Y axis. Grids have been developed on the rotated pole coordinated system where the pole and top left center (TLC) coordinates are (198.0, 39.25) and (331.79, 21.67) respectively. CM files have NETCDF extension and cannot be read in a straightforward way. Hence, to retrieve data and visualize grid points, some operations are needed. For this purpose, the Climate Data Operator, CDO version 1.9.3 installed on the Linux-based distribution system Ubuntu 18.04 LTS, is used in this study where the main operations refer to some actions as follows:

i) Limiting the boundary of CMs' horizontal grids to the bounds of the Chiese catchment (Limune Sul Grada, Gardone Val Trompia, Casa Pirli and Brescia weather station coordinates)
ii) Making the CM files readable and openable
iii) Reading the data and visualizing the grid points within the Chiese catchment

Having applied the three abovementioned actions to CMs files, the user can easily find the coordinates of grid points within the catchment. In this regard, 28 grid points are located within the Chiese domain among which only nine grid points are within the catchment border shown in the Figure 3.2, generated by Lat Lon Digitize toolbox in the QGIS software with the version 3.18.2. Every grid point within the catchment border represents a fictitious weather station, called node in the figure, playing the main role in the hydrological analysis of the catchment and in the CM performance evaluation. Table 3.3 gives the geographical coordinates of the fictitious stations. In our study, all the climate models show the grid points with the same coordinates for both hydro-climatological properties, temperature, and precipitation. In this regard, Peres et al. (2020) stated that climate models may have different grids due to the different origins and the orientation of the axis. Hence, it is worth introducing an evaluation method to RCMs giving knowledge about the suitability of RCMs grid schemes to the configuration of catchment.

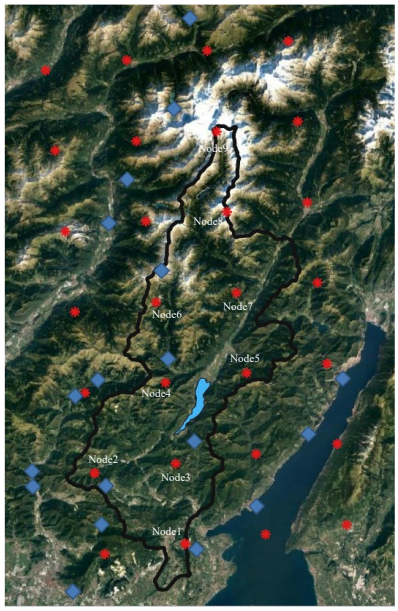

Figure 3.2. The grid points of the RCMs (red stars) in the Chiese domain. Blue diamonds refer to the real gauge rainfall stations

Table 3.3. Coordinates of CMs nodes based on EPSG:4326 Coordinate Reference System

Fictitious Station ID	X (degree)	Y (degree)
1	10.4789	45.5868
2	10.3068	45.6850
3	10.4629	45.6963
4	10.4468	45.8057
5	10.6033	45.8168
6	10.4307	45.9151
7	10.5875	45.9262
8	10.5716	46.0357
9	10.5557	46.1451

3.3.2 Climate Models' Performance Evaluations

The gridded observational-based daily dataset over the Europe domain called E-OBS is used against CMs outputs to evaluate the performance of all 10 current study's regional CMs. For this, the last version of E-OBS was downloaded from the source: https://surfobs.climate.copernicus.eu/dataaccess/access_eobs.php#datafiles for both precipitation and temperature data over a 30 years control period, years 1971 to 2000. The lowest spatial resolution of E-OBS data is chosen which equals 0.10 ° and the E-OBS grid points are visualized within the selection domain which have the same coordinates for both temperature and precipitation data (Figure 3.3). As can be seen, 12 E-OBS fictitious stations are located within the catchment border (see coordinates in Table 3.4). Due to the higher resolution of E-OBS data, the number of E-OBS grid points is larger than that of CM points within the catchment boundaries.

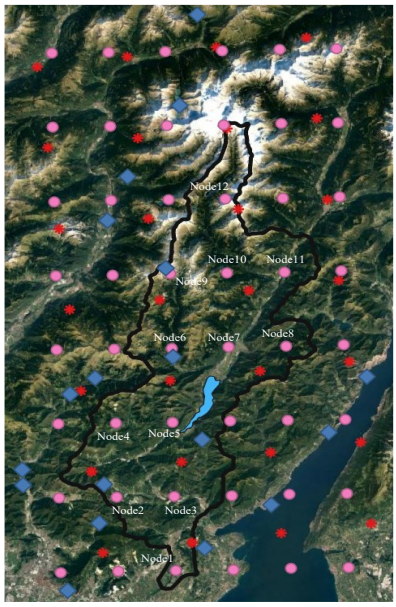

Figure 3.3. The grid points of the E-OBS (pink circles) in the Chiese domain. Blue diamonds and red stars refer to the real gauge rainfall stations and CMs grid points. E-OBS grid points within the catchment are called nodes.

Table 3.4. Coordinates of E-OBS nodes within the Chiese catchment based on EPSG:4326 Coordinate Reference System

Fictitious Station ID	X (degree)	Y (degree)
1	10.4499	45.5499
2	10.3499	45.6499
3	10.4499	45.6499
4	10.3499	45.7499
5	10.4499	45.7499
6	10.4499	45.8499
7	10.5499	45.8499
8	10.6499	45.8499
9	10.4499	45.9499
10	10.5499	45.9499
11	10.6499	45.9499
12	10.5499	46.0499

To evaluate the CMs' performance, the monthly cumulative precipitation and monthly average temperature values are the target variables. The monthly values of CMs are accessible directly from the source, while the daily E-OBS data should be aggregated over the month scale. In this study, the precipitation and temperature variables are represented by $x_{i,j}$ and $y_{i,j}$ where i:1,2,3…,12 and j:1,2,3, …,30 refer to the number of months and years. For every specific month and year, for example i=1 (January) and j=1 (year 1971), the current methodology introduces a variable which gives the weighted average catchment value for the two target variables estimated by Equations (3.1) and (3.2).

$$X_{i,j,catchment} = \sum_{k=1}^{n_f} w_k x_{i,j,k} \tag{3.1}$$

$$Y_{i,j,catchment} = \sum_{k=1}^{n_f} w_k y_{i,j,k} \tag{3.2}$$

where n_f represents the number of fictitious stations within the catchment which are nine and 12 for the CMs and E-OBS data, w_k refers to the weight of every node calculated by the Thiessen polygons method such that the ratio of the Thiessen polygon area associated with the node to the total area of the catchment gives the weight of corresponding node. The weights not only specify the significance role of grid points in the hydrological analysis of the catchment but also evaluate the suitability of CMs numerical schemes to the layout of the catchment in case they have different grid schemes. Moreover, the method marks a difference from most of the other works in the scientific literature, in which the comparison is carried out at the scale of the single grid nodes where the two different resolutions of observations and RCMs should be matched.

Figure 3.4 and Table 3.5 show the Thiessen polygons and area information together with the weights of the fictitious stations for both CMs and E-OBS dataset.

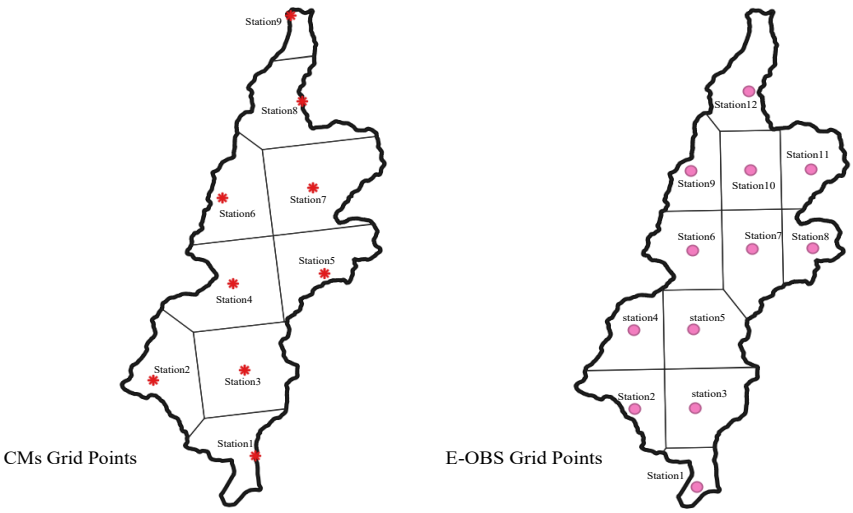

Figure 3.4. The Thiessen polygons of fictitious stations of CMs and E-OBS data, the left and right

Table 3.5. The Thiessen polygon area of fictitious stations together with their weights

	E-OBS		CMs	
Factitious Station ID	**Thiessen Polygon Area (km^2)**	**Weight**	**Thiessen Polygon Area (km^2)**	**Weight**
1	32.82	0.034	77.14	0.079
2	73.53	0.076	101.95	0.105
3	106.06	0.109	146.69	0.151
4	76.35	0.079	144.89	0.149
5	112.00	0.115	104.70	0.108
6	91.52	0.094	102.30	0.105
7	101.80	0.105	159.84	0.165
8	56.44	0.058	109.40	0.113
9	66.00	0.068	24.10	0.025
10	86.18	0.089		
11	76.79	0.079		
12	91.52	0.094		
Summation	971.01	1.00	971.01	1.00

Root Mean Square Error (RMSE) is the statistical index used for estimating the performance of the climate models. It is calculated after ordering the climate model and E-OBS data associated with the benchmark period of n_{years} in ascending order, with the objective to evaluate the extent to which the cumulative frequency of cumulative rainfall and temperature values obtained from the generic climate model is close to the corresponding cumulative frequency of the E-OBS data. For every specific month i, let's say i=1, the monthly error for a given CM for the precipitation and temperature values are calculated by Equations (3.3) and (3.4) as follows:

$$RMSE^{P}_{i,catchment,z}=\sqrt{\frac{\sum_{j=1}^{n_{years}}(X^{E\text{-}OBS}_{i,catchment}-X^{CM}_{i,catchment})^{2}}{n_{years}}} \tag{3.3}$$

$$RMSE^{T}_{i,catchment,z}=\sqrt{\frac{\sum_{j=1}^{n_{years}}(Y^{E\text{-}OBS}_{i,catchment}-Y^{CM}_{i,catchment})^{2}}{n_{years}}} \tag{3.4}$$

where $RMSE^{P}_{i,catchment,z}$ and $RMSE^{T}_{i,catchment,z}$ represent the CM error for simulating month i catchment precipitation and temperature values for climate model z, respectively; n_{years} defines the number of years in the control period which is 30 in the current study; $X^{E\text{-}OBS}_{i,catchment}$ and $X^{CM}_{i,catchment}$ stand for E-OBS and climate model month i precipitation values, respectively; $Y^{E\text{-}OBS}_{i,catchment}$ and $Y^{CM}_{i,catchment}$ represent E-OBS and climate model month i temperature values calculated over the catchment. Representative performance errors of the climate model z where z varies from one to 10, are obtained for precipitation and temperature variables by Equations (3.5) and (3.6):

$$CM^{P}_{z,error}=\frac{\sum_{i=1}^{12}RMSE^{P}_{i,catchment}}{n_{months}} \tag{3.5}$$

$$CM^{T}_{z,error}=\frac{\sum_{i=1}^{12}RMSE^{P}_{i,catchment}}{n_{months}} \tag{3.6}$$

where $CM^{P}_{z\ error}$ and $CM^{T}_{z\ error}$ represent the error of the climate model z in terms of precipitation and temperature simulations, respectively. Indeed, they are equal to the average of all monthly values simulation errors. Finally, n_{months} represents the number of months in a year, which is 12.

After finding the errors of all the CMs, the climate models are ranked based on the relative error for precipitation (Equations (3.7)) and absolute error for the temperature

data (Equations (3.6)). This relative error is defined because the error variance for precipitation is much higher than the one for temperature.

$$CM^{P}_{z,r\_error}=\frac{CM^{P}_{z,error}}{\sum_{z=1}^{n_{CMs}} CM^{P}_{z,error}} \tag{3.7}$$

where, CM^{P}_{z,r_error} stands for the relative error of specific climate model z for the precipitation property and n_{CMs} defines the number of climate models which is 10 in the current study. Climate model ranks in both terms of precipitation and temperature are summed to obtain a rank index number. The climate model with the least total rank index number would be the best model for climate simulation and projection on the Chiese catchment.

3.3.3 Projection and Climate Change Assessment

Using the best suited climate model to the catchment, this study projects the monthly catchment precipitation and temperature values for the 70s decade in the future (2071-2080) and compares the projected data with the corresponding ones related to the 90s decade in the historic period (1991-2000). All generated data by the best climate model are modified by the bias correction factors to make all the simulations reliable. There are many methods for the estimation of bias correction factors (Teutschbein and Seibert 2012); this study uses the linear-scaling method whose main advantage is parsimony. According to this method, the CM monthly precipitation data are corrected by multiplicative factors that bring the monthly means of corrected precipitation to match their observed values in the benchmark past period. On the other hand, the temperature data are adjusted through an additive term that brings the corrected average monthly mean temperature to equal the observed values in the benchmark past period. Thus, the corrections are the followings for precipitation and temperature, respectively:

$$\alpha_{P,i,catchment}=\frac{\overline{(P^{h}_{E\text{-}OBS})_{i,catchment}}}{\overline{(P^{h}_{CM})_{i,catchment}}} \quad i=1,2,3\ldots,12 \tag{3.8}$$

$$\Delta_{T,i,catchment}=\overline{(T^{h}_{E\text{-}OBS})_{i,catchment}}-\overline{(T^{h}_{CM})_{i,catchment}} \quad i=1,2,3\ldots,12 \tag{3.9}$$

where P denotes precipitation and T temperature, the overline indicates the mean operation, the subscript *E-OBS* indicates observed values and subscript h stands for "historic period" (i.e., 1991-2000 in this study); $i=1, \ldots, 12$ is the month index. The corrected historic and future data are given by the following equations:

$$(P'^{f}_{CM})'_{i,j,catchment} = \alpha_{P,i,catchment} \cdot (P^{f}_{CM})_{i,j,catchment} \quad (3.10)$$

$$(T'^{f}_{CM})'_{i,j,catchment} = \Delta_{T,i,catchment} + (T^{f}_{CM})_{i,j,catchment} \quad (3.11)$$

$$(P'^{f}_{CM})'_{i,j,catchment} = \alpha_{P,i,catchment} \cdot (P^{f}_{CM})_{i,j,catchment} \quad (3.12)$$

$$(T'^{f}_{CM})'_{i,j,catchment} = \Delta_{T,i,catchment} + (T^{f}_{CM})_{i,j,catchment} \quad (3.13)$$

where, in addition to previously declared symbols, prime stands for "corrected value", superscript *f* indicates a future period (2071-2080 in this study) and j=1,2, …, 10 is the year index.

Climate change assessment includes finding the trends of corrected precipitation and temperature monthly values as time goes by. For this, the mentioned values of the Chiese catchment are investigated for the three scenarios of greenhouse gas emission, 2.6, 4.5, and 8.5 over the 70s decade in the future and the results are compared with the corresponding ones related to the 1991-2000 decade in the historic period. Additionally, rainfall event characteristics including duration, intensity and depth are assessed and compared. To accomplish this, the hourly data from the best suited climate model are downloaded and modified by the bias correction factors. Independent rainfall events have been selected based on an inter event time $\Delta t_{threshold}$ of about 11 hours, estimated based on the concentration time of the catchment (Giandotti 1933). Figure 3.5 shows the time axis of three independent events where every event takes n hours starting from time t_0 and ending to time t_n. While $t_{0,k}$-$t_{n,k-1} > \Delta t_{threshold}$ and $t_{0,k+1}$-$t_{n,k} > \Delta t_{threshold}$, all the time differences within the event k and other subsequent events would be smaller or equal to the threshold. As the result, the duration, intensity, and depth of event k are estimated by Equations (3.14), (3.15) and (3.16).

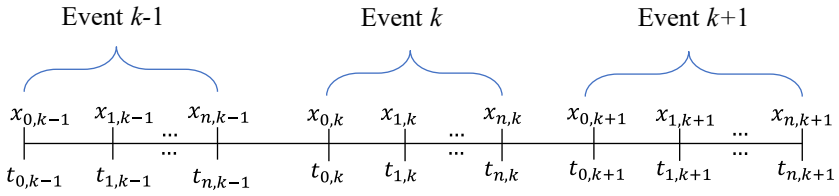

Figure 3.5. The time axis of three independent rainfall events

$$L_k = t_{n,k} - t_{0,k} \tag{3.14}$$

$$D_k = \sum_{i=0}^{n} x_{i,k} \tag{3.15}$$

$$I_k = \frac{D_k}{L_k} \tag{3.16}$$

where, L_k, D_k, I_k represent the length (hours), depth (mm) and intensity (mm/hours) of rainfall event k. Here, the minimum temporal rainfall resolution is one hour which is the main assumption in the current study as the sub hourly temporal resolution for the precipitation data is not provided by the climate models.

Having been calculated, rainfall event lengths, depths and intensities are compared between the three future scenarios and the historic period based on the cumulative frequency distribution graphs.

3.4 COUPLING CLIMATE MODEL WITH THE HYDROLOGICAL MODEL

To couple the climate model with the hydrologic model, the outputs of the climate models, precipitation, and temperature data, are used as the inputs of the hydrologic model. To accomplish this, the Chiese catchment has been modeled through the TOPKAPI software where the input variables and the parameters for the hydrologic model adjustments and simulations are controlled and inserted through the TOPKAPI user interface windows. The main receiver input windows are shown in the Figure 3.6 where the climate model outputs are assembled into the Weather Stations and Monthly Temperature windows (detailed information of every window is provided in the Appendix). As observed, two modules referring to hydrologic and climate models are

linked only by two windows in the TOPKAPI Inputs Interface to complete coupling process. The Weather Stations window include the information on rain gauge and thermometer stations including their coordinates, elevation and hourly data values and the Monthly Temperature contains the stations' monthly average values for solving evapotranspiration equations over the hydrologic simulation period.

The fictitious stations are reconstructed in the Chiese catchment through MapWindow GIS of TOPKAPI. The coordinates and elevation of fictitious stations are obtained from the climate model file source and digital elevation model data. This is another important feature of current methodology where there is no need for matching the spatial resolutions of an RCM and hydrological model through an interpolation method to complete the coupling process.

The hourly precipitation and temperature data are captured from the best climate model. All the inserted data values are modified by bias correction factors before assembling. The coupling process is repeated for the past decade 1991-2000, and for the decade 2071-2080 considering greenhouse gas emission scenarios 2.6, 4.5, and 8.5 to estimate and compare the hydrological components of the catchment including water discharge, percolation, and evapotranspiration. The input variables in the Weather Stations and monthly Temperature windows are changed simulation by simulation while other parameters, such as the soil kinds and land uses, are assumed constant and invariable during the simulations.

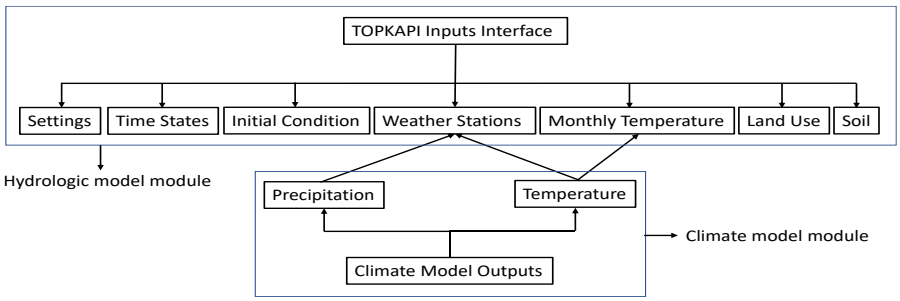

Figure 3.6. Coupling hydrologic and climate models

4. RESULTS

4.1 CLIMATE MODEL RANKINGS

Table 4.1 compares the errors and ranks of the RCMs used for simulating the precipitation and temperature of Chiese catchment where $Rank_P$ and $Rank_T$ represent the ranks of CMs in terms of precipitation and temperature; Ranks Sum is the summation of precipitation and temperature ranks.

Overall, it can be seen that Had-RACM is the best suited model to the Chiese catchment for precipitation simulation, while Nor-HIRH has the best performance for temperature simulation. In terms of total rank number index, Had-RCA4 has the least value, which is five, and it is chosen as the best model for simulating the historic and projected scenarios data in this case study.

Table 4.1. The errors and ranks of climate models for Chiese catchment

Model ID	Model Name	CM^{P}_{z,r_error}	$Rank_P$	$CM^{T}_{z,error}(c^{\circ})$	$Rank_T$	Ranks Sum.
1	CM5-RCA4	12%	6	4.00	6	12
2	IPS-RCA4	11%	5	2.93	4	9
3	Had-RCA4	8%	3	2.38	2	5
4	Had-RACM	5%	1	3.19	5	6
5	MPI-RCA4	12%	6	2.38	2	8
6	ECE-RACM	6%	2	4.71	8	10
7	ECE-RACMr12	6%	2	4.85	9	11
8	ECE-HIRH	17%	8	2.45	3	11
9	ECE-RCA4	10%	4	4.04	7	11
10	Nor-HIRH	13%	7	1.33	1	8

After selecting the best CM, the outputs of CM should be modified by bias correction factors for climate change assessment and use in the hydrological model. Table 4.2 shows the monthly bias correction factors calculated for the Chiese catchment case study.

Table 4.2. The monthly-based CM bias correction factors for Chiese case study

	Bias correction factors	
Month	**Precipitation**	**Temperature (C°)**
January	0.51	4.47
February	0.52	3.83
March	0.60	3.60
April	0.59	2.31
May	0.56	2.58
Jun	0.67	1.21
July	0.93	1.20
August	0.95	0.52
September	0.77	1.80
October	0.77	2.36
November	0.40	1.02
December	0.39	2.20

4.2 CLIMATE CHANGE TRENDS AND IMPACTS ON THE CATCHMENT

Figure 4.1 illustrates variation in the weighted average Chiese catchment precipitation and temperature variables estimated over the two decades in the historic (1991-2000) and future (2071-2080) periods where the impacts of three scenarios, 2.6, 4.5, and 8.5 is evident on the catchment.

Overall, what stands out from the graphs is that there is a catchment warming over time intensified by increase in the greenhouse gas emissions, whereas there is not a clear trend for the precipitation values.

Looking at the details, as regards temperature, the coldest (December) and warmest (July) months remain the same over time. In this regard, the average monthly temperature in July is 18.85° for the 90s decade and significantly raises to 21.40° for the 70s decade with scenario 2.6 (2.55° warming). On the same trend, comparing the historic and future July average temperature, there are remarkable rises for scenarios 4.5 and 8.5, which are from 18.85° to 23.40° (4.55° warming) and from 18.85° to 24.17° (5.32°) respectively.

With respect to the coldest month, there is a considerable catchment warming. While the average monthly temperature is just above 1° for 90s, this raises to 3.41° (roughly 2.41° warming), 6.26° (approximately 5.26° warming), and 6.85 (approximately 5.85° warming)

for scenarios 2.6, 4.5 and 8.5 respectively, indicating in agreement with the warmest month that the scenario 8.5 is the most critical one.

In terms of monthly precipitation for the Chiese catchment, there is not a clear trend and therefore other precipitation's characteristics are investigated for both historic and future data. Figure 4.2 shows the Gumbel cumulative frequency distribution of three characteristics of rainfall events: depth, duration, and intensity for 90s and 70s. As observed, the future rainfall events would be with higher intensity and shorter duration over the Chiese catchment in comparison with the corresponding events over the 90s decade occurred due to the increase in the greenhouse gas emissions. On the opposite, there is not a bold difference in the rainfall event depth behavior between the future and historic climate of Chiese.

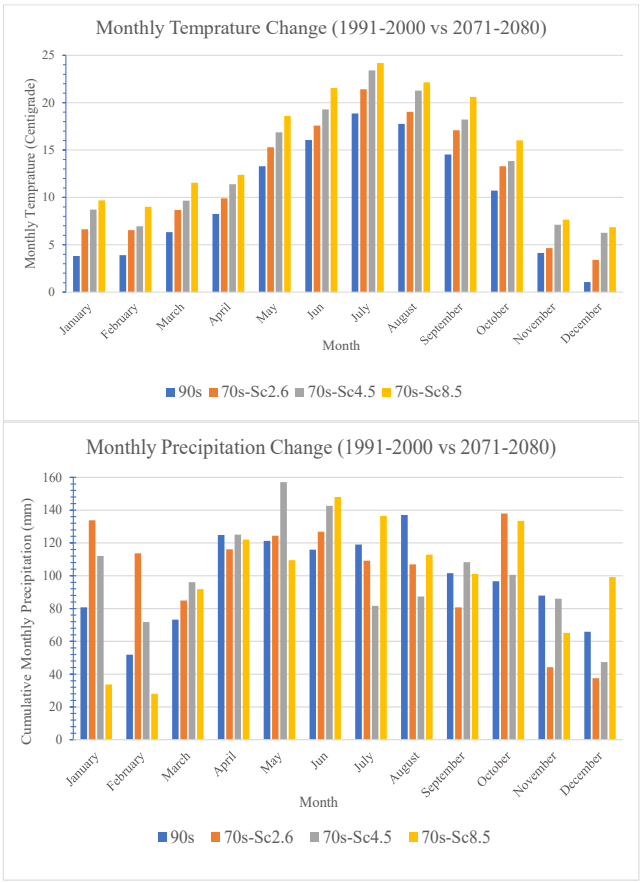

Figure 4.1. Temperature and precipitation changes in the Chiese catchment, Sc is the abbreviation of Scenario

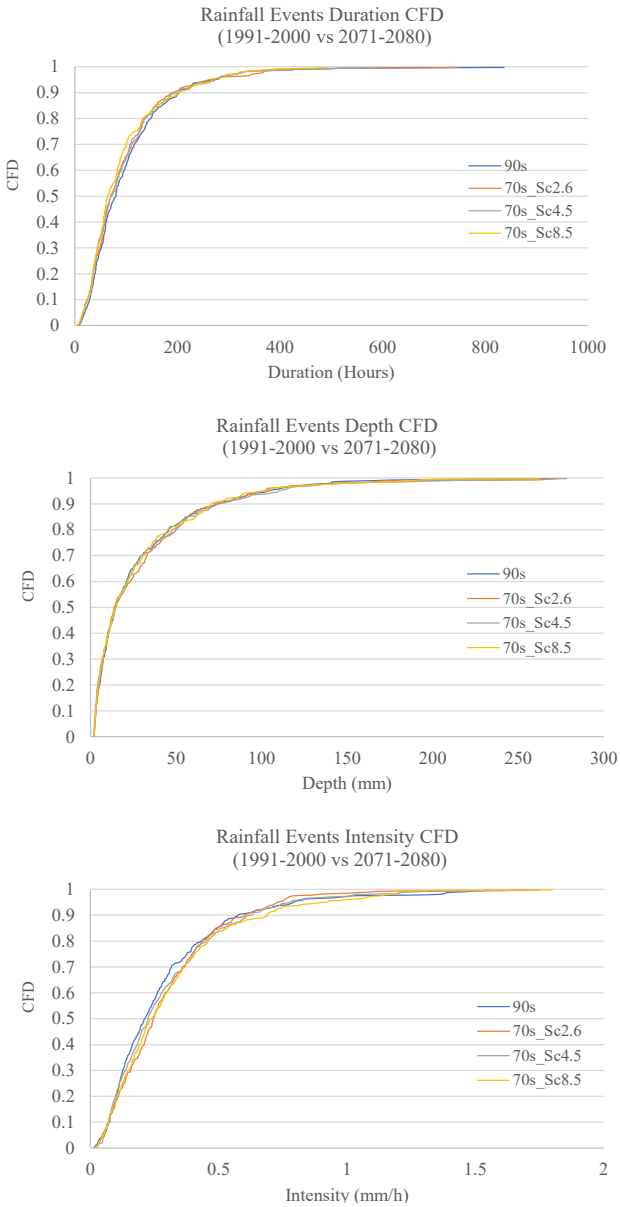

Figure 4.2. The rainfall event characteristics, duration, depth, and intensity for the historic and future periods of Chiese catchment

4.3 HYDROLOGIC MODEL OUTPUTS

Table 4.3 shows and compares the important water balance components at Gavardo station for the four simulations, calculated through TOPKAPI. As can be seen, the precipitation values for future period (2071-2080) simulations are higher than the corresponding one for the historic period (1991-2000) simulation. However, this does not refer to a considerable difference and therefore it is expected that Chiese catchment will not face high variations in the total yearly rainfall depth. As regards the percolation values, future period simulations have a lower value than historic simulation, due to the increase in the temperature values over the Chiese catchment. In this regard, scenario 8.5 has the least value with 494.28 mm, which is about 10% lower than the one related to the 90s simulation with 554.67 mm. Scenario 2.6 doesn't make considerable decrease in comparison to other scenarios with only 0.3% percolation decrease. In agreement, the evapotranspiration values grow for increasing greenhouse gas emission, where scenario 8.5 is the most critical one with 21% increase (from 2619.13 mm to 3178 mm).

Table 4.3. Hydrologic Water Balance components of Chiese catchment over the historic and future periods, 1991-2000 vs 2071-2080

Simulation Name	Precipitation (mm)	Discharge (mm)	Percolation (mm)	Evapotransipation (mm)
90s	11729.29	9130.33	554.67	2619.13
70s_Sc2.6	12162.96	9534.48	552.78	2764.94
70s_Sc4.5	12190.20	9512.52	541.21	2894.41
70s_Sc8.5	11803.40	8750.77	494.28	3178.16

For a better assessment of discharge variations, besides Table 7, Figure 9 compares the cumulative frequency distribution of the yearly maximum discharge for the historic and future decades. Consistently with the trend observed for precipitation intensity, an increase in the catchment maximum discharge is expected for the future. While the increase is appreciable but not exorbitant for the maximum discharge values with CFD lower than 0.8, this is dramatically amplified for anomalies (values with CFD>0.8) of scenarios 2.6 and 4.5.

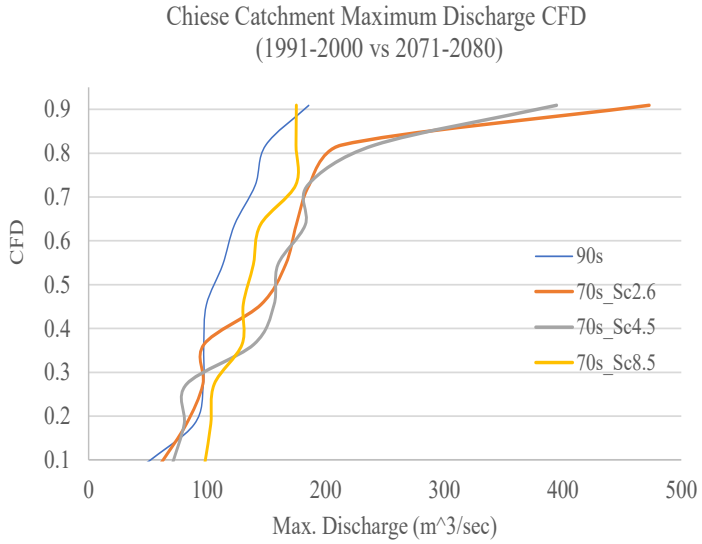

Figure 4.3. The yearly maximum discharge CFD for Chiese catchment over the historic and future periods

5. SUMMARY AND CONCLUSION

Current study attempted to assess the hydrology of river Chiese catchment contributed by regional climate models (RCMs) and observed data. For this, 10 coupled CMs captured from EURO CORDEX initiative and experimented in CMPI5, were chosen. The CMs were evaluated by simulating two hydro-climatological variables, precipitation, and temperature, and comparing the results with the high-resolution E-OBS data. To accomplish this, this study proposed a novel method through which the outputs of climate and E-OBS models, stored on grid points inside the catchment, were compared without any post processing actions on the data such as interpolation (rescaling, remapping, and re-gridding). For this, every grid point, within the boundary of the catchment, was considered as a fictitious weather station with a certain weight impact on the catchment. The weights of fictitious stations were calculated through Thiessen polygons method which is an important step for evaluating the suitability of CMs based on configurations fitting between the layouts of CMs numerical scheme and catchment when CMs have different grid schemes. Moreover, through this method, the significant level of each grid point was recognized and those with low weights played a less important role in the hydrological output of the catchment than the ones with high weights. Following this method and calculating RMSE index for all the CMs, it was proved the Had-RCA4 has the best performance for simulating the monthly precipitation and temperature of the Chiese catchment with the total rank index number equal to five (Table 4.1). It is worth mentioning that Had-RCA4 might not perform as successful as current study for other case studies like the one presented in (Peres et al. 2020), Sicily and Calabria regions in the south of Italy, and therefore selecting the best-performing RCM is highly case dependent.

To couple the CM and hydrologic model, the output of the best climate model (precipitation and temperature) was inserted as the input to the hydrological model developed by TOPKAPI software. This was done at a very fine temporal resolution (1 hour) where there was no need for matching the spatial resolutions between the RCM and hydrological model as every fictitious station of RCM was reconstructed in the Chiese catchment through MapWindow GIS of TOPKAPI. Eventually, four simulations were carried out for the periods, 1991-2000 and 2071-2080 with the scenarios 2.6, 4.5 and 8.5. Hence, the results of Chiese climate change and impact model were as follows:

- While the monthly catchment warming is obvious by all scenarios, there is not a clear trend for monthly precipitation values.
- The warmest and coldest months remain the same for Chiese catchment by climate change scenarios which are July and December respectively. In December, scenarios 8.5 and 2.6 could bring the most and least monthly temperature increase to Chiese catchment with approximately 5.85° and 2.41° warming respectively.
- It is expected that the rainfall events for 70s in the future will occur with higher intensity and shorter duration than the ones for 90s in the historic period, whereas a relevant difference for precipitation depth is not expected.
- Hydrologic outputs for the mentioned simulations showed rises in the catchment decade precipitation, discharge, and evapotranspiration values over 80 years; on the opposite, percolation will be decreased by scenarios where scenario 2.6 does not make high difference with 0.3% change (In any case the detected decreasing percentages do not exceed 10%).

REFERENCES

Adeniyi, M. O. and K. A. Dilau (2018). "Assessing the link between Atlantic Niño 1 and drought over West Africa using CORDEX regional climate models." Theoretical and applied climatology **131**(3): 937-949.

Bentsen, M., I. Bethke, J. B. Debernard, T. Iversen, A. Kirkevåg, Ø. Seland, H. Drange, C. Roelandt, I. A. Seierstad and C. Hoose (2013). "The Norwegian Earth System Model, NorESM1-M–Part 1: description and basic evaluation of the physical climate." Geoscientific Model Development **6**(3): 687-720.

Bosshard, T., M. Carambia, K. Goergen, S. Kotlarski, P. Krahe, M. Zappa and C. Schär (2013). "Quantifying uncertainty sources in an ensemble of hydrological climate-impact projections." Water Resources Research **49**(3): 1523-1536.

Brigode, P., L. Oudin and C. Perrin (2013). "Hydrological model parameter instability: A source of additional uncertainty in estimating the hydrological impacts of climate change?" Journal of Hydrology **476**: 410-425.

Chen, J., F. P. Brissette and R. Leconte (2011). "Uncertainty of downscaling method in quantifying the impact of climate change on hydrology." Journal of hydrology **401**(3-4): 190-202.

Chen, J., F. P. Brissette and P. Lucas-Picher (2015). "Assessing the limits of bias-correcting climate model outputs for climate change impact studies." Journal of Geophysical Research: Atmospheres **120**(3): 1123-1136.

Christensen, O. B., M. Drews, J. H. Christensen, K. Dethloff, K. Ketelsen, I. Hebestadt and A. Rinke (2007). "The HIRHAM regional climate model. Version 5 (beta)."

Collins, W., N. Bellouin, M. Doutriaux-Boucher, N. Gedney, P. Halloran, T. Hinton, J. Hughes, C. Jones, M. Joshi and S. Liddicoat (2011). "Development and evaluation of an Earth-System model–HadGEM2." Geoscientific Model Development **4**(4): 1051-1075.

Di Virgilio, G., J. P. Evans, A. Di Luca, R. Olson, D. Argüeso, J. Kala, J. Andrys, P. Hoffmann, J. J. Katzfey and B. Rockel (2019). "Evaluating reanalysis-driven CORDEX regional climate models over Australia: model performance and errors." Climate Dynamics **53**(5): 2985-3005.

Diasso, U. and B. J. Abiodun (2017). "Drought modes in West Africa and how well CORDEX RCMs simulate them." Theoretical and Applied Climatology **128**(1-2): 223-240.

Doss-Gollin, J., D. J. Farnham, M. Ho and U. Lall (2020). "Adaptation over Fatalism: Leveraging High-Impact Climate Disasters to Boost Societal Resilience." Journal of Water Resources Planning and Management **146**(4): 01820001.

Dufresne, J.-L., M.-A. Foujols, S. Denvil, A. Caubel, O. Marti, O. Aumont, Y. Balkanski, S. Bekki, H. Bellenger and R. Benshila (2013). "Climate change projections using the IPSL-CM5 Earth System Model: from CMIP3 to CMIP5." Climate dynamics **40**(9): 2123-2165.

Ehret, U., E. Zehe, V. Wulfmeyer, K. Warrach-Sagi and J. Liebert (2012). "HESS Opinions" Should we apply bias correction to global and regional climate model data?"." Hydrology and Earth System Sciences **16**(9): 3391-3404.

Endris, H. S., P. Omondi, S. Jain, C. Lennard, B. Hewitson, L. Chang'a, J. Awange, A. Dosio, P. Ketiem and G. Nikulin (2013). "Assessment of the performance of CORDEX regional climate models in simulating East African rainfall." Journal of Climate **26**(21): 8453-8475.

Foley, A. and I. Kelman (2018). "EURO-CORDEX regional climate model simulation of precipitation on Scottish islands (1971–2000): model performance and implications for decision-making in topographically complex regions." International Journal of Climatology **38**(2): 1087-1095.

Frei, C., J. H. Christensen, M. Déqué, D. Jacob, R. G. Jones and P. L. Vidale (2003). "Daily precipitation statistics in regional climate models: Evaluation and intercomparison for the European Alps." Journal of Geophysical Research: Atmospheres **108**(D3).

Giandotti, M. (1933). Previsione delle piene e delle magre dei corsi d'acqua.

Giorgetta, M. A., J. Jungclaus, C. H. Reick, S. Legutke, J. Bader, M. Böttinger, V. Brovkin, T. Crueger, M. Esch and K. Fieg (2013). "Climate and carbon cycle changes from 1850 to 2100 in MPI-ESM simulations for the Coupled Model Intercomparison Project phase 5." Journal of Advances in Modeling Earth Systems **5**(3): 572-597.

Giorgi, F., L. O. Mearns, C. Shields and L. McDaniel (1998). "Regional nested model simulations of present day and 2× CO 2 climate over the central plains of the US." Climatic Change **40**(3): 457-493.

Hazeleger, W., C. Severijns, T. Semmler, S. Ştefănescu, S. Yang, X. Wang, K. Wyser, E. Dutra, J. M. Baldasano and R. Bintanja (2010). "EC-Earth: a seamless earth-system prediction approach in action." Bulletin of the American Meteorological Society **91**(10): 1357-1364.

Iversen, T., M. Bentsen, I. Bethke, J. Debernard, A. Kirkevåg, Ø. Seland, H. Drange, J. Kristjansson, I. Medhaug and M. Sand (2013). "The Norwegian earth system model, NorESM1-M–Part 2: climate response and scenario projections." Geoscientific Model Development **6**(2): 389-415.

Jacob, D., J. Petersen, B. Eggert, A. Alias, O. B. Christensen, L. M. Bouwer, A. Braun, A. Colette, M. Déqué and G. Georgievski (2014). "EURO-CORDEX: new high-resolution climate change projections for European impact research." Regional environmental change **14**(2): 563-578.

Kotlarski, S., K. Keuler, O. B. Christensen, A. Colette, M. Déqué, A. Gobiet, K. Goergen, D. Jacob, D. Lüthi and E. Van Meijgaard (2014). "Regional climate modeling on European scales: a joint standard evaluation of the EURO-CORDEX RCM ensemble." Geoscientific Model Development **7**(4): 1297-1333.

Kunstmann, H., K. Schneider, R. Forkel and R. Knoche (2004). "Impact analysis of climate change for an Alpine catchment using high resolution dynamic downscaling of ECHAM4 time slices." Hydrology and Earth System Sciences **8**(6): 1031-1045.

Lenderink, G., A. Buishand and W. van Deursen (2007). "Estimates of future discharges of the river Rhine using two scenario methodologies: direct versus delta approach." Hydrol. Earth Syst. Sci. **11**(3): 1145-1159.

Liu, Z. and E. Todini (2002). "Towards a comprehensive physically-based rainfall-runoff model." Hydrol. Earth Syst. Sci. **6**(5): 859-881.

Mascaro, G., D. D. White, P. Westerhoff and N. Bliss (2015). "Performance of the CORDEX-Africa regional climate simulations in representing the hydrological cycle of the Niger River basin." Journal of Geophysical Research: Atmospheres **120**(24): 12425-12444.

Mengistu, A. G., T. A. Woldesenbet and Y. T. Dile (2021). "Evaluation of the performance of bias-corrected CORDEX regional climate models in reproducing Baro–Akobo basin climate." Theoretical and Applied Climatology **144**(1): 751-767.

Park, C., S.-K. Min, D. Lee, D.-H. Cha, M.-S. Suh, H.-S. Kang, S.-Y. Hong, D.-K. Lee, H.-J. Baek and K.-O. Boo (2016). "Evaluation of multiple regional climate models for summer climate extremes over East Asia." Climate Dynamics **46**(7-8): 2469-2486.

Peres, D. J., R. Modica and A. Cancelliere (2019). "Assessing Future Impacts of Climate Change on Water Supply System Performance: Application to the Pozzillo Reservoir in Sicily, Italy." Water **11**(12): 2531.

Peres, D. J., A. Senatore, P. Nanni, A. Cancelliere, G. Mendicino and B. Bonaccorso (2020). "Evaluation of EURO-CORDEX (Coordinated Regional Climate Downscaling Experiment for the Euro-Mediterranean area) historical simulations by high-quality observational datasets in southern Italy: insights on drought assessment." Natural Hazards and Earth System Sciences **20**(11): 3057-3082.

Schmidli, J., C. Goodess, C. Frei, M. Haylock, Y. Hundecha, J. Ribalaygua and T. Schmith (2007). "Statistical and dynamical downscaling of precipitation: An evaluation and comparison of scenarios for the European Alps." Journal of Geophysical Research: Atmospheres **112**(D4).

Seaby, L. P., J. C. Refsgaard, T. Sonnenborg and A. Højberg (2015). "Spatial uncertainty in bias corrected climate change projections and hydrogeological impacts." Hydrological Processes **29**(20): 4514-4532.

Senatore, A., S. Hejabi, G. Mendicino, J. Bazrafshan and P. Irannejad (2019). "Climate conditions and drought assessment with the Palmer Drought Severity Index in Iran: evaluation of CORDEX South Asia climate projections (2070–2099)." Climate Dynamics **52**(1): 865-891.

Senatore, A., G. Mendicino, G. Smiatek and H. Kunstmann (2011). "Regional climate change projections and hydrological impact analysis for a Mediterranean basin in Southern Italy." Journal of Hydrology **399**(1-2): 70-92.

Smiatek, G. and H. Kunstmann (2019). "Simulating future runoff in a complex terrain alpine catchment with EURO-CORDEX data." Journal of Hydrometeorology **20**(9): 1925-1940.

Smiatek, G., H. Kunstmann and A. Senatore (2016). "EURO-CORDEX regional climate model analysis for the Greater Alpine Region: Performance and expected future change." Journal of Geophysical Research: Atmospheres **121**(13): 7710-7728.

Stone, M. C., R. H. Hotchkiss, C. M. Hubbard, T. A. Fontaine, L. O. Mearns and J. G. Arnold (2001). "IMPACTS OF CLIMATE CHANGE ON MISSOURI RWER BASIN WATER YIELD 1." JAWRA Journal of the American Water Resources Association **37**(5): 1119-1129.

Strandberg, G., L. Bärring, U. Hansson, C. Jansson, C. Jones, E. Kjellström, M. Kupiainen, G. Nikulin, P. Samuelsson and A. Ullerstig (2015). CORDEX scenarios for Europe from the Rossby Centre regional climate model RCA4, SMHI.

Tariku, T. B., T. Y. Gan, J. Li and X. Qin (2021). "Impact of Climate Change on Hydrology and Hydrologic Extremes of Upper Blue Nile River Basin." Journal of Water Resources Planning and Management **147**(2): 04020104.

Teutschbein, C. and J. Seibert (2010). "Regional climate models for hydrological impact studies at the catchment scale: a review of recent modeling strategies." Geography Compass **4**(7): 834-860.

Teutschbein, C. and J. Seibert (2012). "Bias correction of regional climate model simulations for hydrological climate-change impact studies: Review and evaluation of different methods." Journal of hydrology **456**: 12-29.

Teutschbein, C. and J. Seibert (2012). "Bias correction of regional climate model simulations for hydrological climate-change impact studies: Review and evaluation of different methods." Journal of Hydrology **456-457**: 12-29.

Um, M. J., Y. Kim and J. Kim (2017). "Evaluating historical drought characteristics simulated in CORDEX East Asia against observations." International Journal of Climatology **37**(13): 4643-4655.

van Meijgaard, E., L. Van Ulft, W. Van de Berg, F. Bosveld, B. Van den Hurk, G. Lenderink and A. Siebesma (2008). The KNMI regional atmospheric climate model RACMO, version 2.1, Citeseer.

Van Uytven, E. and P. Willems (2018). "Greenhouse gas scenario sensitivity and uncertainties in precipitation projections for central Belgium." Journal of Hydrology **558**: 9-19.

Vezzoli, R., P. Mercogliano, S. Pecora, A. L. Zollo and C. Cacciamani (2015). "Hydrological simulation of Po River (North Italy) discharge under climate change scenarios using the RCM COSMO-CLM." Science of The Total Environment **521-522**: 346-358.

Voldoire, A., E. Sanchez-Gomez, D. S. y Mélia, B. Decharme, C. Cassou, S. Sénési, S. Valcke, I. Beau, A. Alias and M. Chevallier (2013). "The CNRM-CM5. 1 global climate model: description and basic evaluation." Climate dynamics **40**(9): 2091-2121.

Wanielista, M. P. (1990). "Hydrology and water quantity control."

Watterson, I., M. Dix, H. Gordon and J. McGregor (1995). "The CSIRO nine-level atmospheric general circulation model and its equilibrium present and doubled CO2 climates." Australian Meteorological Magazine **44**(2): 111-125.

Wu, F.-T., S.-Y. Wang, C.-B. Fu, Y. Qian, Y. Gao, D.-K. Lee, D.-H. Cha, J.-P. Tang and S.-Y. Hong (2016). "Evaluation and projection of summer extreme precipitation over East Asia in the Regional Model Inter-comparison Project." Climate Research **69**(1): 45-58.

APPENDIX

A.1 TOPKAPI INTRODUCTION

The hydrological model is constructed with the software TOPographic Kinematic APproximation and Integration TOPKAPI, providing high resolution information on the hydrological state of the river Chiese catchment shown in the Figure 3.1. TOPKAPI is a distributed and physically based model, able to reproduce the behavior of the main components of the hydrologic cycle. Beside sub-surface, overland and channel flow, it includes components representing infiltration, percolation, evapo-transpiration (ET), and snowmelt (Figure A.1). In TOPKAPI, each catchment cell is structured in three layers, namely superficial soil, deeper soil, and aquifer. Each layer is modelled as a non-linear reservoir while the flow is approximated through the kinematic wave model.

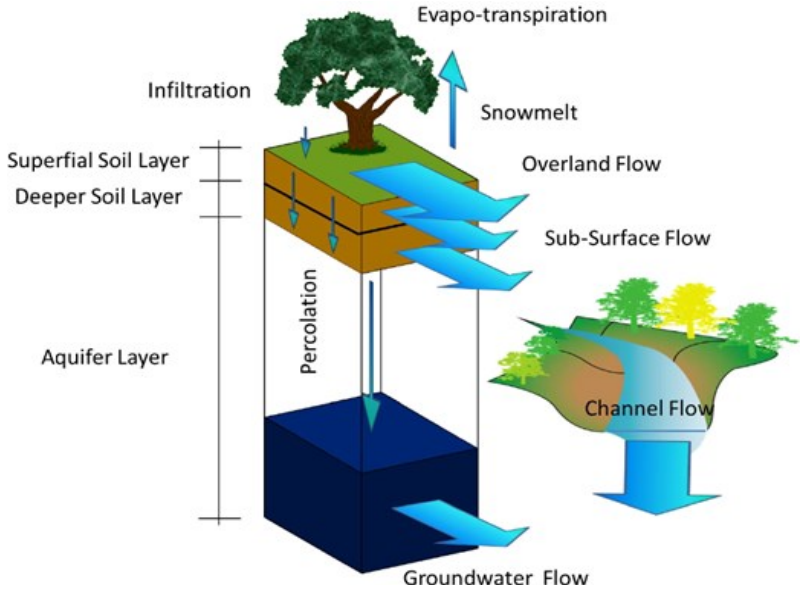

Figure A.1. Conceptual layout of TOPKAPI

A.2 HYDROLOGICAL MODELLING OF CHIESE CATCHMENT

To complete the hydrologic modelling of Chiese catchment, three phases are followed: 1- Pre- Processors Work, 2- Parameters Settings, 3- Calibration.

A.2.1 Pre-Processors Work

The aim of this initial phase is to build the GIS based project of the hydrological model TOPKAPI on the Chiese catchment area. To do this, some thematic maps, and shapefiles as input layers in the software GIS, called MapWindow, are provided:

- Shapefile of the catchment area
- Digital Elevation Model
- Map of the soil units (shapefile or raster)
- Map of the land use units (shapefile or raster)
- Shapefile of the river network
- Shapefile of the lakes
- Shapefile of the gauged stations (thermometers, rain gauges and hydrometers)

The catchment of the river together with the river network are constructed starting from the Digital Elevation Model of the area (Figure A.2). At the end of this phase the pre-processors have implemented all the input information and created the scheme of the catchment. In this step, the catchment is discretized into cells with a prefixed size, in each of which the equations of the model are applied for every time step of the simulation. Hence, for each cell, the soil unit, the elevation, the land use unit, the slope, the channel components, and the initial conditions are defined. The maps of soil kind are used to characterize the territory of the catchment.

For each cell, the input information about temperature and precipitation are provided to calculate the water discharge. Every cell can receive the water discharge from the upstream cells (max three for four dimensions model, max seven for eight dimensions model) and give discharges only to its downstream cell. The connections between cells occur along the line of maximum slope, calculated based on the cell elevation. The hierarchy of the channels in the network of rivers is also shown in Figure A.3.

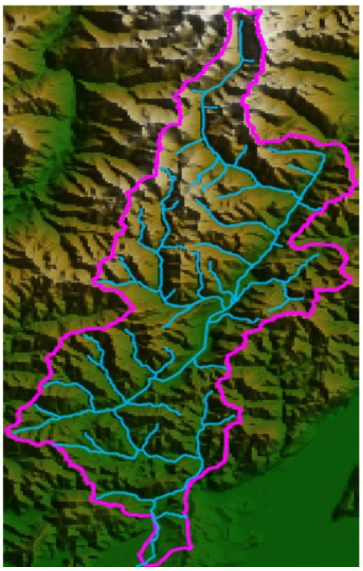

Figure A.2. Water network and DEM of the Chiese catchment

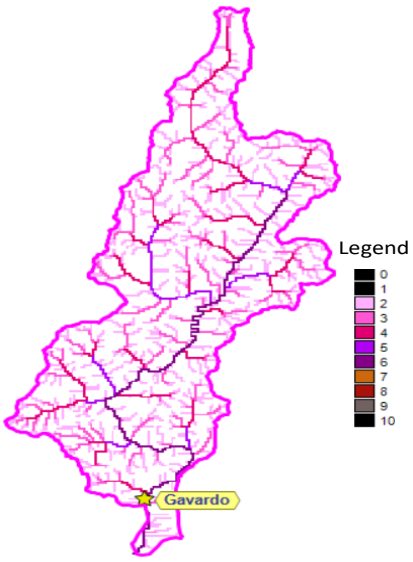

Figure A.3. Map of hierarchy of the channel network (the darker color corresponds to a higher degree in the hierarchy). The star sign represents the hydrometer of Gavardo station

A.2.2 Parameters' Settings

Once the pre-processor work is done, the parameters values are set to run the first simulation. There are many parameters to be set like soil, snow, evapotranspiration, channel routing, land use, and reservoirs parameters. Soil, land use and monthly temperature could have many parameters if there are many different soil units, land use units and thermometers in the catchment area. Hence, they are imported from external csv tables. The soil parameters have more impact in the evaluation of the water discharges during flood events than the other parameters. Their first values can be calculated with standard pedo-transfer functions that considers the texture and percentage soil component of every soil unit. Once all the parameters and the input meteorological data are set, there should be a decision about the time step and the time of the first simulation.

A.2.3 Calibration

Calibration of hydrology model of Chiese catchment is done through comparing the model results of a simulation with measures at Gavardo station where observed discharge data are available. The calibration must be driven on a long period that includes many meteorological events. This is performed in a physically based way, by setting parameters such as the horizontal permeability, saturated and residual water content, soil depth for each kind of present soil (Figures A.4 and A.5)

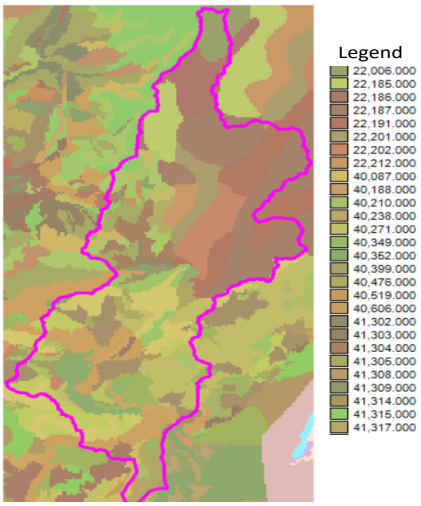

Figure A.4. Map of soil kind; every color is related to a code of a particular soil (shown in the legend) representing different parameters shown in Figure A.5

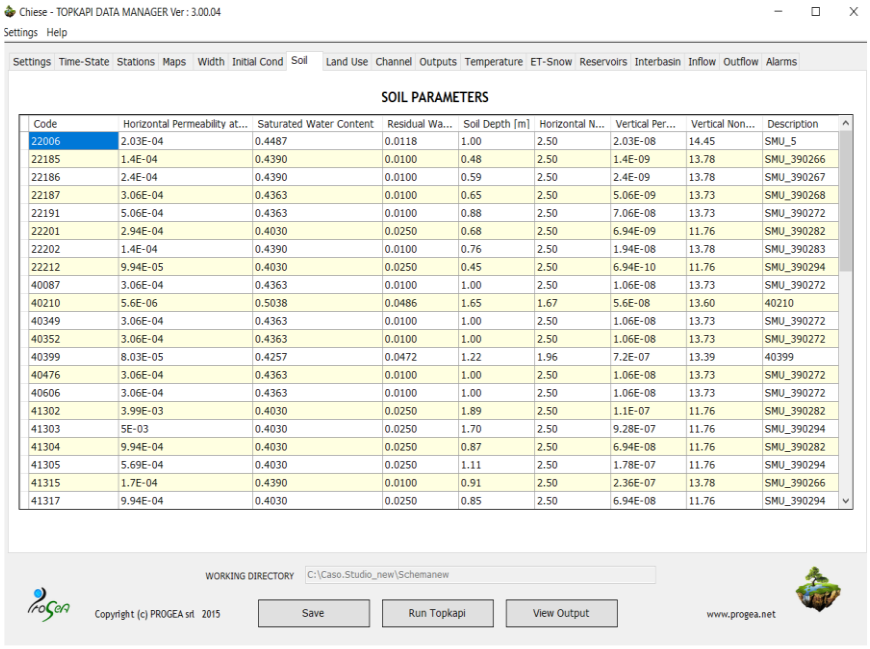

Figure A.5. Output of TOPKAPI for the Chiese catchment. The first graph above shows the fit of simulated to observed water discharge at Gavardo (blue and red graphs indicate the observed and simulated discharges respectively). The other graphs report the other processes of the hydrological cycle, including percolation to groundwaters

(a) ***Calibration Results*** After being calibrated, TOPKAPI is applied for the simulation of the hydrological cycle in the catchment, to reproduce each process (rainfall, runoff, evapotranspiration, infiltration, and flow in the river network) at each cell of the domain. While the real rainfall pattern is used at input, the model performance is examined in terms of capability of reproducing the observed water discharge pattern at the Gavardo station. As Figure A.6 shows, the agreement of the model to the experimental data is very good.

Among the various Outputs of TOPKAPI, the pattern of percolation will be used to analyze groundwater recharge in current scenarios, and in future scenarios obtained by simulating the catchment reply to rainfall patterns obtained from future climate projections.

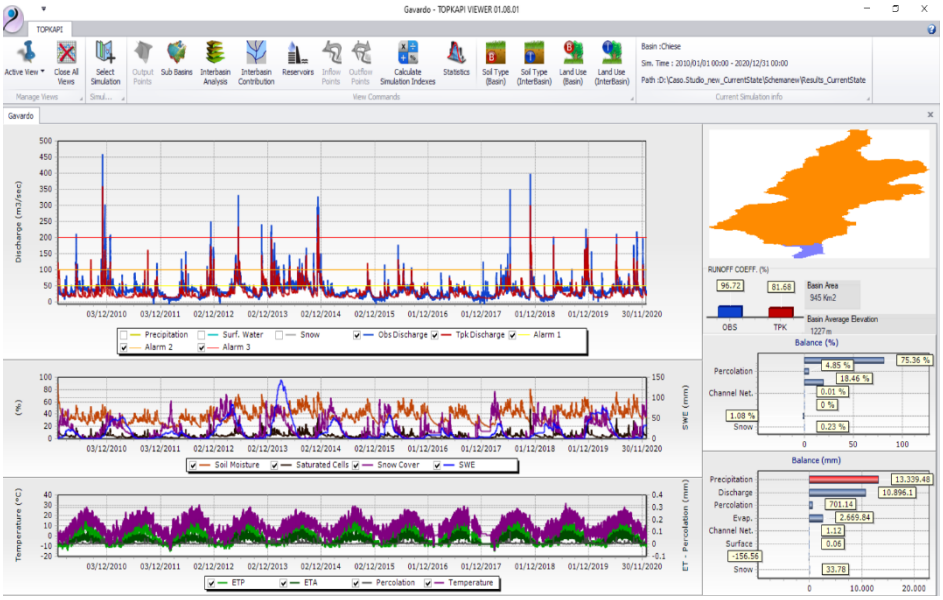

Figure A.6. Output of TOPKAPI for the Chiese catchment. The first graph above shows the fit of simulated to observed water discharge at Gavardo (blue and red graphs indicate the observed and simulated discharges respectively). The other graphs report the other processes of the hydrological cycle, including percolation to groundwaters

(b) ***Calibrated Parameters*** The calibrated parameters as well as input variables for running simulations can be observed in every window of TOPKAPI user interface shown in Figure 3.6 explained in the page 28 of the thesis. Followings indicate the main window values.

In the Settings Windows, TOPKAPI grid, global position, and drainage network information is inserted. As regards the TOPKAPI grid information, the total cells number, cell size, number of columns and rows, X and Y lower left are respectively 15554, 250, 143, 282, 597250m and 5042050m (based on WGS84/UTM Zone 32 coordinate reference system). As for the global position, the latitude and longitude are 45.80 and 10.50 degree. With respect to drainage network info, the number of outlet and flow directions are one and four respectively.

In the Time-State Window, the computation time step length is 60 minutes. The simulation initial and end dates are 01/01/2010 and 31/12/2020 respectively. In the Stations Window, the hourly rainfall and temperature data as well as their stations

coordinates are inserted as external .csv files. The spatialization mode is based on the Inverse Square Distance (ISD) interpolation method with search distance and maximum interpolation distance parameters equal 25000m and 100000m respectively.

The data in the Initial Conditions, Land Use and Temperature Windows are shown in the Figures A.7, A.8 and A.9 respectively. Other Windows information is available upon request.

INITIAL CONDITIONS

Month	Average Soil Mosture	River Level/Width
Jan	0.90	0.01
Feb	0.90	0.01
Mar	0.80	0.01
Apr	0.80	0.01
May	0.70	0.01
Jun	0.60	0.01
Jul	0.60	0.01
Aug	0.60	0.01
Sep	0.70	0.01
Oct	0.80	0.01
Nov	0.90	0.01
Dec	0.90	0.01

Figure A.7. Calibrated data in Initial Conditions Window of user interface TOPKAPI for the Chiese catchment

LAND USE PARAMETERS

Code	Manning Coefficent [s/m^(1/3)]	JAN	FEB	MAR	APR	MAY	JUN	JUL	AUG	SEP	OCT	NOV	DEC	Description
112	0.100	0.40	0.40	0.40	0.40	0.40	0.40	0.40	0.40	0.40	0.40	0.40	0.40	(112) Discontinuous urban fabric
121	0.050	0.20	0.20	0.20	0.20	0.20	0.20	0.20	0.20	0.20	0.20	0.20	0.20	(121) Industrial or commercial units
131	0.050	0.20	0.20	0.20	0.20	0.20	0.20	0.20	0.20	0.20	0.20	0.20	0.20	(131) Mineral extraction sites
211	0.120	0.70	0.90	1.00	1.20	1.25	1.15	0.90	0.80	1.15	1.25	1.20	0.70	(211) Non-irrigated arable land
231	0.060	0.80	1.05	1.10	1.10	1.10	0.80	0.90	0.80	0.80	1.00	1.00	0.90	(231) Pastures
241	0.100	0.70	1.00	1.10	1.20	1.35	1.20	1.10	0.90	1.30	1.25	1.20	0.75	(241) Annual crops associated with permanent crops
242	0.100	0.70	1.00	1.10	1.20	1.35	1.20	1.10	0.90	1.30	1.25	1.20	0.75	(242) Complex cultivation patterns
243	0.200	0.70	1.00	1.10	1.20	1.35	1.20	1.10	0.90	1.30	1.25	1.20	0.75	(243) Land principally occupied by agriculture with significant areas of n...
311	0.280	0.60	0.70	0.95	1.05	1.05	0.80	0.80	0.80	0.80	1.20	1.10	0.60	(311) Broad-leaved forest
312	0.220	0.90	0.90	0.90	0.90	0.90	0.90	0.90	0.90	0.90	0.90	0.90	0.90	(312) Coniferous forest
313	0.280	0.75	1.00	0.90	0.95	1.20	0.85	0.85	0.85	0.85	1.05	1.00	0.75	(313) Mixed forest
321	0.100	0.80	1.05	1.10	1.10	1.10	0.80	0.90	0.80	0.80	1.00	1.00	0.90	(321) Natural grasslands
322	0.100	0.60	0.65	0.70	0.75	0.80	0.80	0.85	0.85	0.85	0.80	0.80	0.60	(322) Moors and heathland
324	0.160	0.75	1.00	0.90	0.95	1.20	0.85	0.85	0.85	0.85	1.05	1.00	0.75	(324) Transitional woodland-shrub
332	0.040	0.20	0.20	0.20	0.20	0.20	0.20	0.20	0.20	0.20	0.20	0.20	0.20	(332) Bare rocks
333	0.070	0.60	0.60	0.60	0.60	0.60	0.60	0.60	0.60	0.60	0.60	0.60	0.60	(333) Sparsely vegetated areas
335	0.030	1.05	1.05	1.05	1.05	1.05	1.05	1.05	1.05	1.05	1.05	1.05	1.05	(335) Glaciers and perpetual snow
512	0.030	1.05	1.05	1.05	1.05	1.05	1.05	1.05	1.05	1.05	1.05	1.05	1.05	(512) Water bodies
6053	0.030	1.05	1.05	1.05	1.05	1.05	1.05	1.05	1.05	1.05	1.05	1.05	1.05	(1053) Lago d'Idro

Figure A.8. Calibrated data in Land Use Window of user interface TOPKAPI for the Chiese catchment

AVERAGE MONTHLY TEMPERATURES

Area Code	Elevation[m]	Area Name	JAN	FEB	MAR	APR	MAY	JUN	JUL	AUG	SEP	OCT	NOV	DEC
4034	2325.00	Pantano d'Avio	-4.29	-3.96	-0.95	2.66	5.38	9.96	12.21	12.42	8.24	4.18	0.39	-2.49
4037	1147.00	Cavacca	0.60	1.15	4.42	8.45	11.48	16.39	18.66	18.29	13.99	9.33	5.29	2.38
4061	399.00	Caino	3.40	4.71	8.78	12.94	15.81	20.56	22.94	22.48	18.36	13.21	8.62	4.28
4087	1128.00	Cevo	1.35	2.04	5.40	9.31	12.13	16.66	18.86	18.51	14.80	10.12	5.92	2.84
6022	780.00	Bagolino	1.49	2.81	5.96	10.43	12.70	17.28	19.44	18.76	15.08	10.70	6.12	2.59
6035	911.00	Bione - San B...	2.55	3.11	6.06	10.37	12.95	18.22	20.59	20.18	15.87	11.27	6.64	4.08
6200	2418.00	Lago della Va...	-4.89	-5.10	-3.14	0.45	2.72	7.54	10.22	9.78	6.47	3.19	-0.65	-2.55
6216	75.00	Limone sul Ga...	6.21	7.63	10.59	14.99	18.07	23.36	25.61	24.97	21.28	16.26	11.23	7.13
6242	1069.00	Memmo	1.63	2.11	4.73	8.83	11.36	16.29	18.63	17.99	14.16	10.01	5.82	3.30
6331	291.00	Puegnago del ...	4.12	6.19	9.48	13.74	16.31	21.56	24.19	23.14	18.90	14.01	9.23	5.18
6374	290.00	Sarezzo-Via d...	2.33	5.38	8.90	13.45	16.30	21.28	23.60	22.63	18.37	13.49	8.24	3.18
6398	374.00	Tignale-Oldesio	4.60	6.31	9.42	13.90	16.74	22.04	24.35	24.07	19.45	14.36	9.56	5.79
6400	70.00	Toscolano	6.01	7.39	10.40	14.91	17.93	23.35	25.97	25.04	21.20	16.14	11.60	6.87

Figure A.9. Calibrated data in Temperature Window of user interface TOPKAPI for the Chiese catchment